

AVO analysis with partial stacking to detect gas anomalies in the GÜEPAJÉ-3D project

Juan C. Mosquera*, Alfredo Ghisays and Luis Montes

Received: March 03, 2012; accepted: April 01, 2013; published on line: June 28, 2013

Resumen

La técnica AVO con apilados parciales se aplicó en un campo gasífero para detectar presencia de gas al tope de la Formación Ciénaga de Oro (FCO) usando apilados parciales del programa sísmico terrestre Güepajé-3D y apoyado con registros del pozo Ayombe-1.

Mediante la técnica de sustitución de fluidos se simuló el reemplazamiento de gas por agua para conocer la sensibilidad de la respuesta sísmica al cambio del fluido en un segmento del pozo Ayombe-1. Se observó una anomalía clase I al tope de la FCO, aun cuando las respuestas de sustituir gas por agua fueron muy similares al aplicar la técnica AVO con apilados parciales se observaron anomalías AVO clase I al tope de la FCO en los pozos con gas Ayombe-1 y Güepajé-1 y ninguna en el pozo seco Güepajé-3. A pesar de tener gas, en el pozo Güepajé-2 los resultados permiten diferenciar entre una incipiente anomalía clase I y ninguna.

Al usarse en el volumen sísmico del Proyecto Güepajé-3D la técnica suministra un mapa de indicador directo de gas que se correlaciona con estructura de la superficie al tope de la FCO.

Pueden factores líticos como compactación, cementación y presencia de carbonatos supra yaciendo la FCO, así como la variabilidad en el espesor variable de las capas parcial y totalmente saturadas al tope de la FCO, generar anomalías en zonas con baja probabilidad de tener gas.

Palabras clave: caso histórico, modelado de pozo, tendencia de fondo, anomalía de AVO, factor de fluido, apilados parciales, Güepajé-3D.

Abstract

We applied analysis AVO with partial stacking to an onshore gas field in order to detect gas at the top of the Ciénaga de Oro formation (FCO), by using seismic gathers of the Güepajé-3D project. The technique was supported by petrophysical analysis of the Ayombe-1 well.

The sensitivity of seismic response to changes in the saturating fluid was evaluated by fluid substitution technique in an interval of the Ayombe-1 well. As a result, a class I AVO anomaly at the top of the FCO was observed, even though the gas and water responses were similar.

After applying AVO with partial stack technique at the top of FCO, AVO class I anomalies were observed in the Ayombe-1 and Güepajé-1 gas wells and none in the dry Güepajé-3 well. In spite of being reported with gas, the results in the Güepajé-2 well indicated any to an incipient class I anomaly related to a weak seismic response associated to gas.

When the technique was applied to the seismic volume of the Güepajé-3D Project, a map of the direct gas indicator was obtained. The map shows a high correlation with the structural surface at top of FCO. Lithic factors such as compaction, cementation and carbonate overlaying the FCO and variable thickness of partial and full saturated layers, may cause anomalies in zones unlikely to contain gas.

Key words: case history, well modeling, background trend, AVO anomaly, fluid factor, partial stacks, Güepajé-3D.

J.C. Mosquera*
Petrobras Colombia Ltd.
Carrera 7 Núm. 71-21. Piso 17
Bogotá, Colombia
*Corresponding author: juanmosque@yahoo.com

A. Ghisays
Universidad del Atlántico
Facultad de Ciencias básicas
Km. 7. Vía Puerto Colombia
E-mail: alfredoghisays@mail.uniatlantico.edu.co

L. Montes
Universidad Nacional de Colombia
Departamento de Geociencias
Carrera 30 Núm. 45 - 03
Ed. Manuel Ancízar, Of. 326
Bogotá, Colombia
E-mail: lamontesv@unal.edu.co

Introduction

The elastic nature of rocks, depends on lithology and fluid content in pores, (Koefoed, 1955; Gassmann, 1951).

Bright spots in stacked sections were associated with gas accumulation, and later extended to related oil anomalies. Hilterman (1975) retook Koefoed's work, by analyzing how amplitude varies with incidence angle before stacking to predict lithology. As in bright spot cases, AVO anomalies were associated to gas but the possibility of using such methodology to indicate the presence of oil was foreseen.

AVO analysis was applied to localize hydrocarbon reserves and to diminish the risk of exploratory projects. Although the number of successful wells increased, dry wells with this type of anomalies were still reported. Ostrander (1984) published a method applied to prestack sections to discern anomalies caused by sandstones with or without gas. Rutherford and Williams (1989) characterized three different seismic anomalies produced by hydrocarbons (class I, phase change class II, and bright spot class III). AVO analysis gained a new impulse with the contributions of Hilterman (1975) and Smith and Gidlow (1987), who established the concepts of Intercept and Gradient, and introduced the analysis of Intercept and Gradient images separately. In the linear relationship between seismic amplitudes and squared sine of reflecting angles, the Gradient represents the slope and the Intercept the reflecting coefficient. Rutherford and Williams (1989) and Castagna (1997), proposed classifying AVO anomalies in four classes according to Intercept and Gradient values. Rosa *et al.* (1999) introduced the Elastic Impedance concept, based on using volumes partially stacked by range of angles together with the visualization and analysis of images of Gradients and Intercept, (Connolly, 1999).

The partial stack technique has been widely applied in elastic and simultaneous inversion to estimate physical properties (Maver and Bolding, 2004) and velocities by constraining the inversion with borelog information (Wei *et al.*, 2006).

AVO with partial stack technique is part of the corporate knowledge in some companies; however, there are no related publications to date. In the study area some confidential AVO studies have been performed using 2D seismic lines. We applied this technique to a seismic volume of the Güepajé-3D project, supported with well log analysis. Some zones with anomalies associated to gas at the top of the FCO were identified. Factors such as compaction, cementation and carbonates in rocks that overlay the FCO, together with variable thickness layers partially or fully

saturated, may cause anomalies in zones with unlikely gas presence.

Location

The Güepajé – Ayombe seismic 3D program is located in an area that includes the municipalities of San Pedro and the Guaimaral and Canutalito police Inspections, in the Department of Sucre, Colombia, as seen on the map in Figure 1.

The seismic dataset covers an area of 112 km², of which, 64 km² are located in the Magangué block, 41 km² in the Ayombe block and 7 km² in La Creciente block. In 1992 gas was discovered in the FCO in the Güepajé-1 well and some gas samples were reported in the Middle Porquero and in the Lower Porquero formations. By the end of 1992 the Ayombe-1 well, drilled at a distance of 6.5 km north of the Güepajé-1 well, reported gas in the FCO (Sánchez, 1993).

In 1993 the Güepajé-2 well was drilled at 2.9km NNW from the Güepajé-1 well, suggesting gas field continuity in the same units of the Güepajé-1 well. By the end of 1993 the Güepajé-3 well was drilled at 5 Km South from the Güepajé-1 well, where the target FCO sandstones were found argillaceous without gas.

Geology

The Lower Magdalena Valley basin (VIM acronym in Spanish) is located in the Northwest of Colombia, where oblique subduction along the Romeral fault system has formed a trans-pressure and trans-tension deformation since the Late Cretaceous to date (Barrero *et al.*, 2008). From top to base, the stratigraphic column in the area contains the formations of Corpa (Pleistocene-Upper Pliocene), Tubará (Upper Miocene), Porquero (Upper and Lower Miocene), Ciénaga de Oro (Oligocene-Lower Miocene) and the basement (Pre Miocene). The Porquero formation is divided in Upper and Lower units with a thin microfossil carbonate level at bottom.

The petroleum system source rock is a very thick shale from Early Miocene (Porquero Lower Formation), rich in both organic material and type II kerogen. The FCO has an upper unit with a high type III organic material content with the generation window in the deepest areas of the basin. The reservoir consists of FCO sandstones and limestones with net thickness around 90 m and 15% of average porosity. The seal rock is formed by the Lower Porquero shales and the FCO shales. The Tubará formation also acts as seal unit. Different types of structural traps emboss the potential of this basin such as traps associated to top closures in faults related to contractions, anticline closings in the lower part of normal

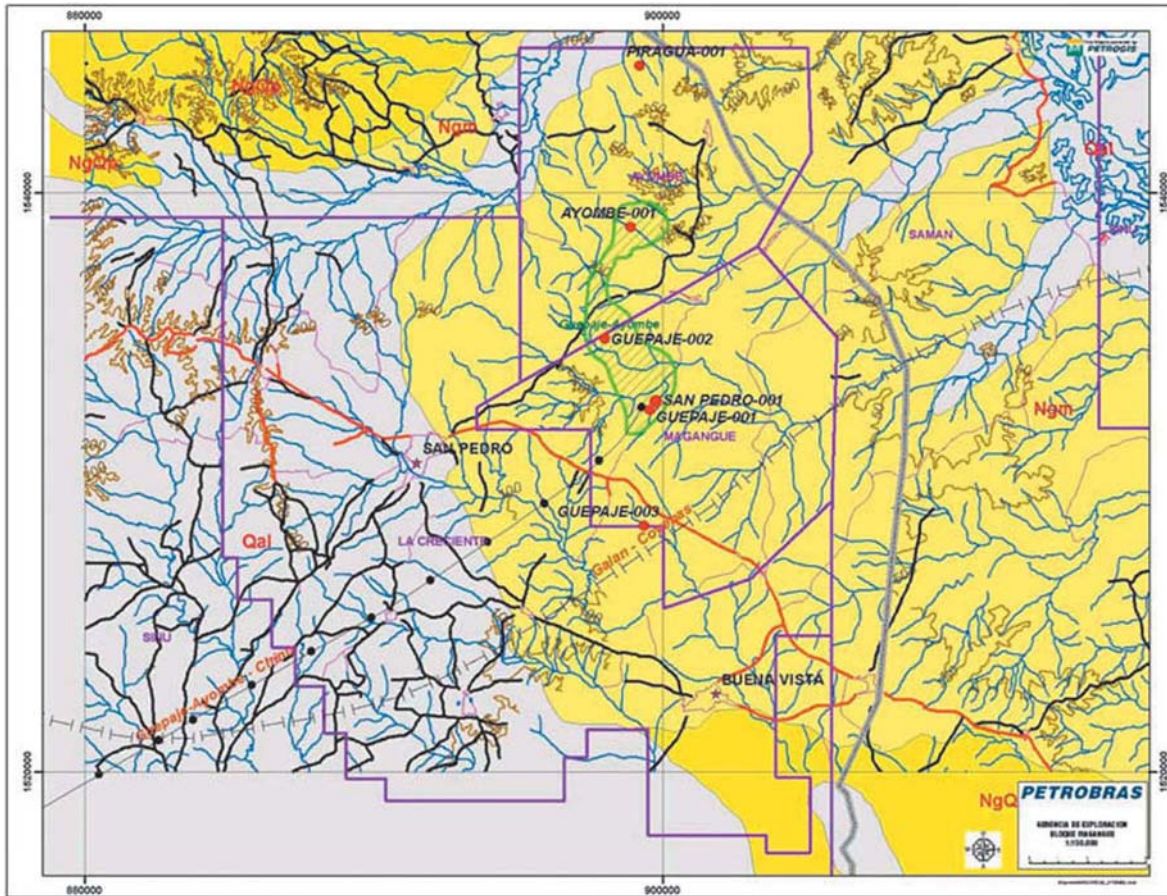


Figure 1. Map of the study area, including Magangué, Ayombe and La Creciente blocks.

faults, structures related to geometries in bloom generated by transpression, and rollovers in the hanging blocks of normal listric faults. Stratigraphic traps are also a potential in carbonate rocks and a submarine range of turbidites.

Active source rocks in generation/expulsion phase are present in an extensive area in the so called Plato sub-basin. The API gravity for oil generated inside the basin varies between 30° to 52°. The sulphur content is too low whereas the paraffin's concentration is relatively high. Several geo-chemical parameters indicate that most of the oil was originated in a relatively dioxic proximal siliciclastic environment. The most probable migration occurred along the network of fractures and faults planes (Barrero *et al.*, 2008).

The tops of the Tubará, Upper and Lower Porquero, Ciénaga de Oro formations and also Basement were interpreted in the migrated sections; such events were tied up with the Ayombe-1 well check shot, as seen in the Figure 2.

In the seismic section, the Corpa formation overlays the Tubará formation which has a moderately variable thickness and presents

medium to strong reflections with parallel to sub-parallel layers dipping to the SWS; its seismic character is consistent with its high sandstones content through the section. The Porquero Superior formation, composed of shales, presents a variable thickness and weak reflectors.

The Ayombe -1 well logs were correlated with the seismic dataset of the Güepajé-3D program, which had a 30m x 30m bin and 30 nominal fold. The seismic volume was processed up to a prestack migrated volume (PSTM) applying a special process sequence for AVO by angles range, the volume was interpreted as seen in the inline of Figure 2. The Figure 3B shows a detailed structural interpretation at the top of the FCO. The FCO has a variable thickness ranging from a few to 200 meters with a 100m thickness average in the area.

Theory

The wave behavior at a discontinuity between two semi infinite elastic media is determined by the Zoeppritz equations, guaranteeing both displacement and stress continuity on the two opposite sides. These equations were approximated by Shuey (1985) through the expression:

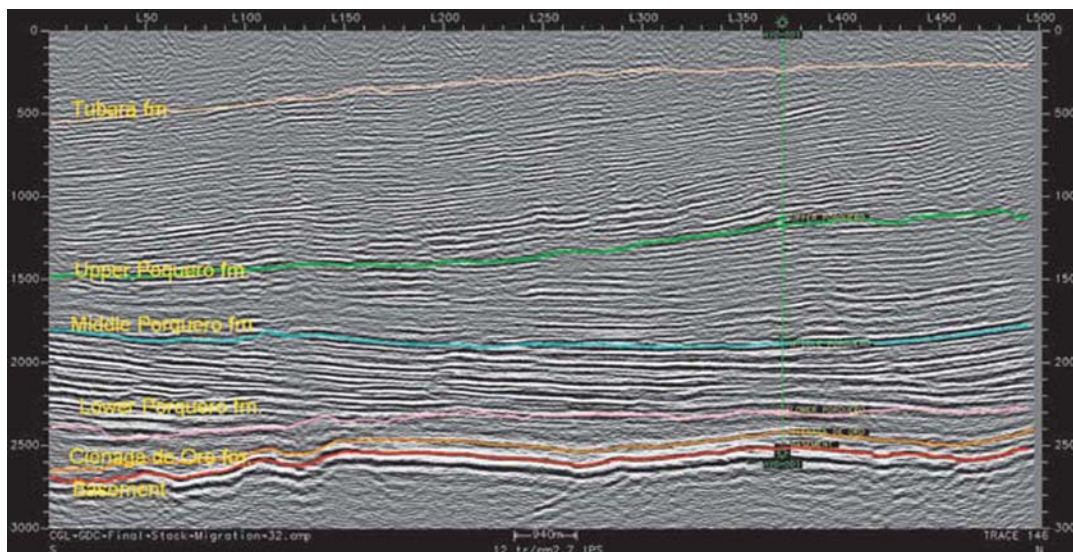


Figure 2. The Tubará, Porquero Superior, Porquero Medio, Porquero Inferior, Ciénaga de Oro formations and Basement, are interpreted from the youngest at the top to the oldest at the bottom.

$$\begin{aligned}
 A(\theta) = & \underbrace{\frac{1}{2} \left(\frac{\Delta V_P}{\alpha} + \frac{\Delta \rho}{\rho} \right)}_{\theta \leq 10^\circ} \\
 & + \underbrace{\left(\frac{1}{2} \frac{\Delta V_P}{\alpha} - 4 \left(\frac{\beta}{\alpha} \right)^2 \frac{\Delta V_S}{\beta} - 2 \left(\frac{\beta}{\alpha} \right)^2 \frac{\Delta \rho}{\rho} \right)}_{\theta \leq 35^\circ} \sin^2 \theta \\
 & + \underbrace{\frac{1}{2} \left(\frac{\Delta V_P}{\alpha} \right) (\tan^2 \theta - \sin^2 \theta)}_{\theta \leq 45^\circ}
 \end{aligned} \tag{1}$$

where ρ is average density, and α and β are P and S wave average velocities, ΔV_S , ΔV_P and $\Delta \rho$ are velocity and density changes from one media to another, θ is the reflection angle and A is the amplitude of the reflected wave. For θ lesser than 35° the equation 1 is approximated to

$$A(\theta) = I + G \sin^2 \theta \tag{2}$$

Where I is the Intercept and is the Gradient. According to equation 2 and in case of near offsets, i.e. $10^\circ < \theta < 20^\circ$, the amplitudes shall be renamed as $A_M(\theta) = I + G \sin^2 \theta_M$. In case of far offsets, i.e. $20^\circ < \theta < 35^\circ$, the amplitudes shall be $A_F(\theta) = I + G \sin^2 \theta_F$.

After manipulating and solving them, the following is obtained:

$$I = A_M - \left(\frac{A_F - A_M}{\sin^2 \theta_F - \sin^2 \theta_M} \right) \sin^2 \theta_N \tag{3}$$

by:

$$G = A_M \left(\frac{1}{\sin^2 \theta_M - \sin^2 \theta_N} \right) - A_N \left(\frac{1}{\sin^2 \theta_F - \sin^2 \theta_M} \right) \tag{4}$$

By using the equations 3 and 4, the Intercept and Gradient are correlated in a section, where the data located along the straight line defines the trend (background) whereas those others are orthogonally deviated to it (Figure 4B). The deviation is used as a fluid factor indicator (Smith & Gidlow, 1987) and is given by:

$$F_F = \frac{\Delta V_P}{\alpha} - M \frac{\beta}{\alpha} \frac{\Delta V_S}{\beta} \tag{5}$$

M corresponds to the slope of the relationship $V_P = 1.16 V_S + 1360$, established by Castagna *et al.* (1984) from sonic and seismic measurements in mudrocks.

Modeling the Ayombe-1 well

In the Ayombe-1 well, the analyzed 2357–3340m interval includes the Lower Porquero and Ciénaga de Oro formations and the Basement, along with which Gamma Ray (GR), Resistivity (HRS), Sonic (DT8D) and Density (RHOB) logs were run. Although the shear velocity log was not acquired in this well, a pseudo shear velocity profile was

calculated by the Greenberg-Castagna method (1992). The complete sets of logs, including the estimated pseudo shear log, are shown in figure 3A.

A well logs analysis in the 2357-3371 m interval provided the following results. The GR log shows a sandstone-shale pattern. The Resistivity log indicates a 40% - 60% gas saturation range in the 3210 to 3228 m interval, a 10% to 20% gas saturations range in the 3228 to 3232 m interval and 100% water saturation between 3232 m and 3362 m deep. In depth, Poisson's relation log tends to decrease but arriving at the top of FCO (gas reservoir at 3210 m) it falls abruptly and rises immediately to continue its former decreasing trend.

The top of FCO is clearly identified by the abrupt changes in Resistivity, GR, Density and Sonic logs as observed in Figure 3A. Observable breaks around 3130 m in GR, Resistivity, Density and Sonic logs tend to point out the top of carbonate level overlaying the FCO.

To match the seismic volume along the well, a synthetic seismogram was obtained by the convolution of a wavelet extracted from the seismic volume with the product of multiplying Sonic by Density logs, after depth to time conversion. The Figure 3B depicts the stack section in the vicinity of the Ayombe-1 well along the 2100 - 2500m interval. It is observed how the seismogram ties the Ciénaga de Oro, the Lower Porquero and part of the Upper Porquero formations.

In the next step, some synthetic seismograms were generated with angles from 0° to 40°

varying each 2°, to observe how the amplitude changes with the reflecting angle. An obtained seismogram is seen in Figure 4A, where amplitude is characterized by a positive intercept (peak) that decreases with an angle (negative gradient) at the top of the FCO fm. Using seismic data at the top of FCO in the vicinity of the well, the Intercept-Gradient cross plot was generated (Figure 4B).

The linear regression through data clustered in the upper polygon defines the background or the non anomalous data. The estimated straight line, with a slope of 1.156, intercepts the abscissa in 0.0015. The points which are not aligned with the background are considered anomalous, i.e. those ones within the below irregular hexagon, are identified as a class I anomaly.

This kind of anomaly characterizes layers overlaying lower impedance rocks that might generate dim spots in stacked section because hydrocarbon reduces the reservoir - seal impedance contrast.

The fluids substitution was simulated in the 3210-3228 m interval (40% - 60% gas saturated) and the 3232-3362 m interval (100% water saturated), using the Biot - Gassmann equations. The obtained responses in both cases are characterized by negative Gradients and positive Intercepts, although the amplitudes are always higher in the 100% water saturation case than in the partially saturated gas case, as noted in Figure 5. The Gamma Ray, Resistivity, Density, Vs and Vp responses, in both the partially and fully saturated cases, are shown in Figure 6.

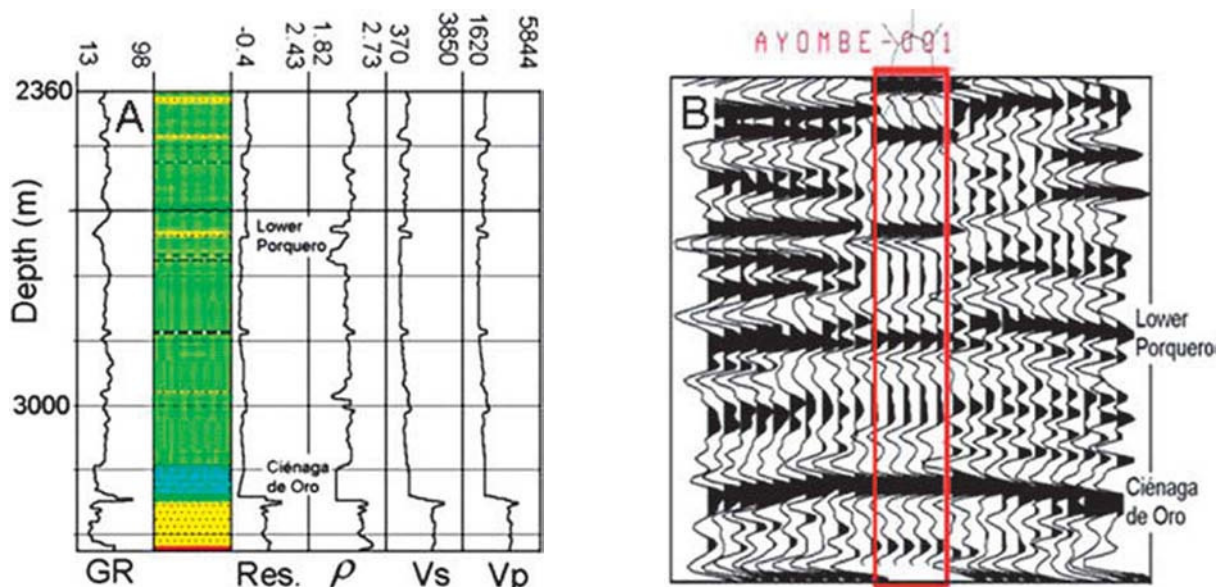


Figure 3. A) The Interval of 2357m of depth to the bottom of the Ayombe-1 well with borehole logs. B) The synthetic seismograms in the inset tie up the seismic section.

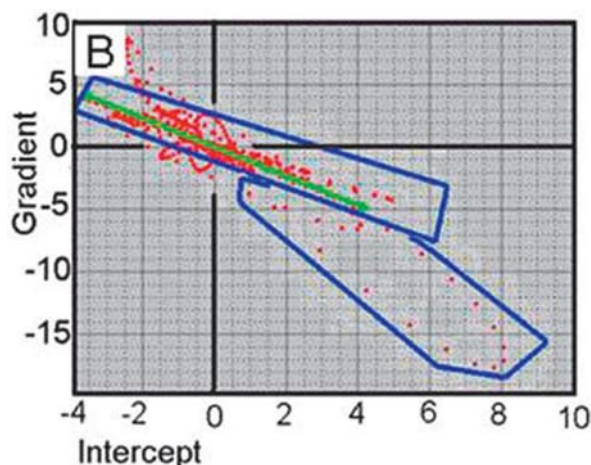
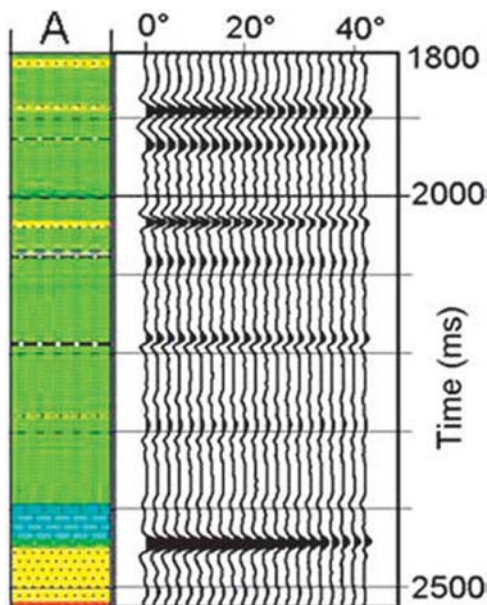


Figure 4 A) At the top of the FCO fm. the amplitude decreases with the angle. B) Data in the IV quadrant indicates a class I anomaly at the top of the FCO fm.

In the 100% water saturation case, when water fills up pores in rock matrix at the top of FCO, the following was observed. The Gamma Ray log remains unchanged because its response does not depend on fluids in pores. The Resistivity log falls quickly due to the gas is more resistive than water. The Density log increases because water is denser than gas. The shear velocity remains the same because liquids cannot be sheared, whereas acoustic wave velocity increases due to the fact that liquids are not compressible.

The 33m of seismic resolution at 3200m depth impedes to discriminate the transition zone with 80%-90% gas saturation and with a 23m thickness. Therefore, the top of the fully saturated water zone cannot be picked out. Besides, possible tuning related to absence of frequencies at far offsets might increase the uncertainty.

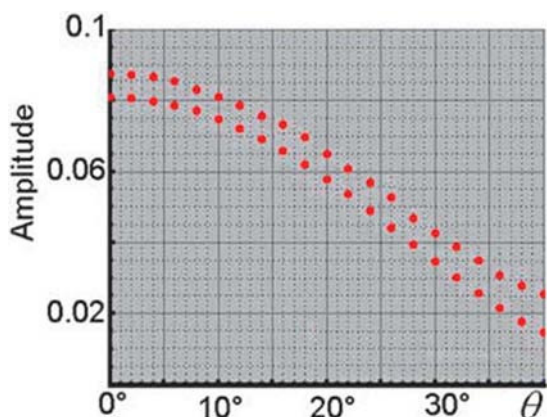


Figure 5. In the partially and fully saturated cases, at the top of the FCO, the amplitude decreases with the angle.

Partial stack AVO analysis

The partial stacks of near offsets (0°-10° range angle), mid offsets (10°-20°) and far offsets (20°-37°) were initially generated. Although, the near offset stack was not considered in this analysis because of the very low signal to noise ratio. The obtained partial stacks together with stacking velocities were used to calculate the Gradient (Figure 7A) and the Intercept (Figure 7B) sections.

In order to restrict the analysis at the top of the FCO, only those data inside the boxes of figures 7A and 7B were correlated. As a result, the obtained cross correlation graph was inserted in Figure 8A. Using the same straight line that established the background at the top of the FCO, an orthogonal deviation section was generated, Figure 8B. At the top of the FCO in the vicinity of Ayombe-1 well a green color and a tiny red color are observed (indicated by an arrow), which according buttons at right of Figure 8B indicates IV to III quadrant and hence a weakly class II to a class I anomaly. This result agrees with the result obtained by

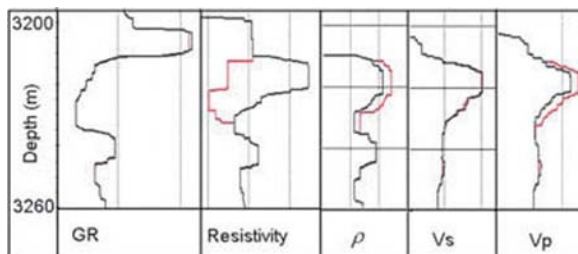


Figure 6. Logs at the top of FCO partially (in black) and fully saturated (in red) cases.

previous well modeling. This partial stack AVO methodology was applied to seismic traces belonging to three 2D seismic lines that crossed or were very close to the three wells Güepajé-1 (line 160), the Güepajé-2 (line 244) and the Güepajé-3 (line 28). Consequently, the three deviation sections associated to the mentioned lines were obtained, focusing on target zones in vicinities of the three considered wells. The analysis of the deviation sections of the line 160 at top of FCO in Güepajé-1 well (indicated by an arrow) identified III to IV quadrant pointing out a class II to a class I anomaly (Figure 9A). In the deviation section of the line 244 at the top of the FCO in Güepajé-2 well (marked with an arrow) no anomaly was identified Figure 9B. Finally an incipient class I anomaly was detected in the deviation section of the line 28 in the Güepajé-3 well, see the arrow in Figure 9C. Up to this point, the partial stack AVO methodology has been applied to 2D seismic data and after having verified its robustness with well logs, the technique was used on 3D seismic volume to detect anomalies associated to gas over the surface defining the top of the FCO.

The mid and far offset stacks at the top of the FCO surface previously obtained were used

to generate the Intercept (Figure 10A) and the Gradient (Figure 10B) maps associated to this surface. In the Intercept map, positive values are observed in the vicinity of the Ayombe-1 (>0.249), Güepajé-1 (>0.436), Güepajé-2 (>0.037) and Güepajé-3 (>0.096) wells, with color ranging from green to brown in the colors scale. In the Gradient map negative values are observed in zones around the locations of the four considered wells. The values of -4.66 for Ayombe-1, -0.40 for Güepajé-1, -1.88 for Güepajé-2 and -1.29 for Güepajé-3 ($\gg -1.29$) wells are associated to colors ranging from white to red. The anterior results, and the Gradient and Intercept values around wells, are in agreement with those supplied by the petrophysical analysis and the 2D seismic analysis formerly done. In both maps the 2480 ms contour line highlights the gas-water contact (GWC) obtained by extrapolating these contacts in the wells.

Finally, an orthogonal deviation map used as a fluid indicator map was obtained, in Figure 11, using as reference background the same straight line established for the Ayombe-1 well. In this map, anomalous values are indicated by colors ranging from green to red. It is notable the

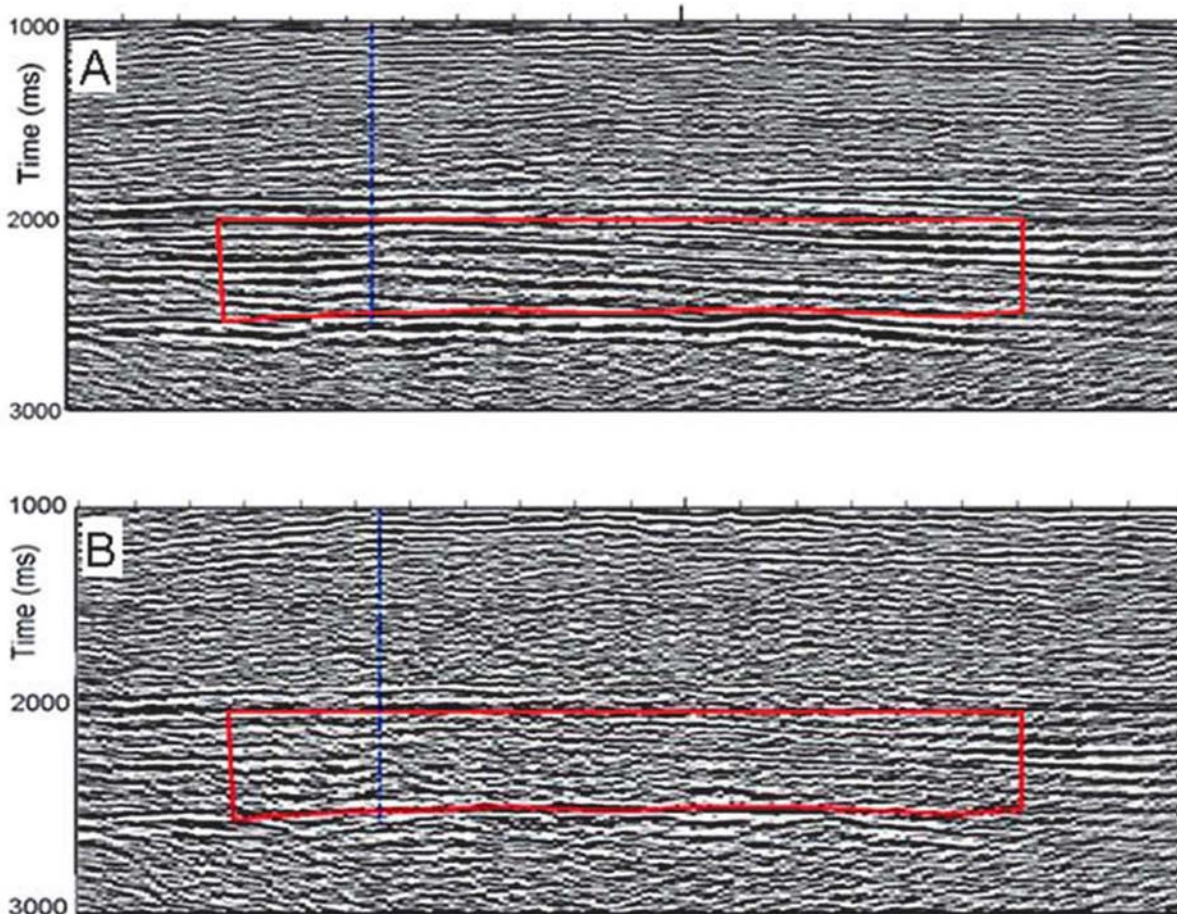


Figure 7. In the Line 370, the polygon surrounds the target in A) the mid offset stack and B) the far offset stack.

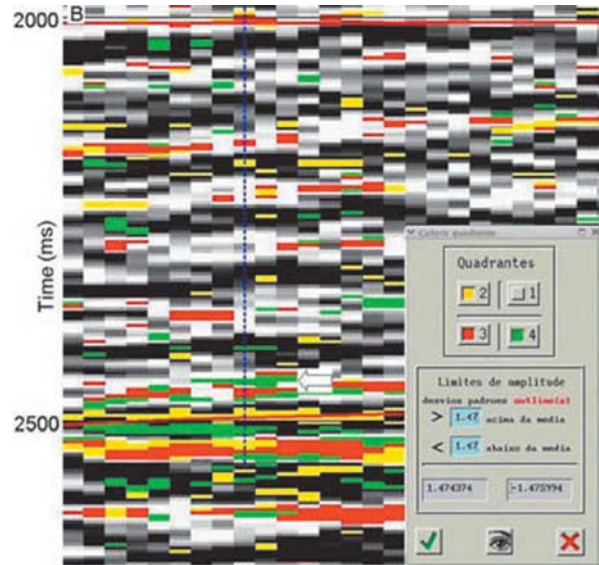
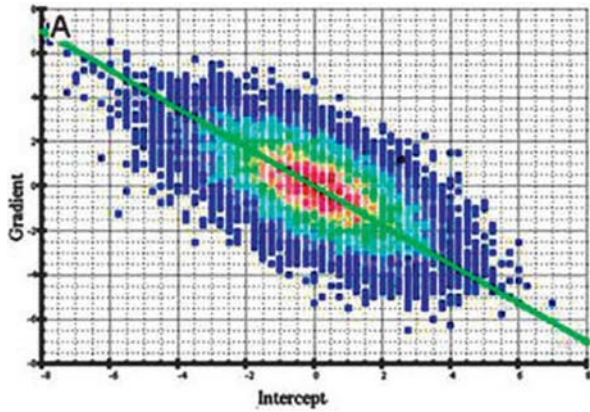


Figure 8. A) Gradient vs. Intercept cross plot B) In the orthogonal deviation section, at the top of FCO (by a white arrow) in the Ayombe-1 well (in blue) a green color is observed indicating a 4th AVO quadrant and hence a class I anomaly.

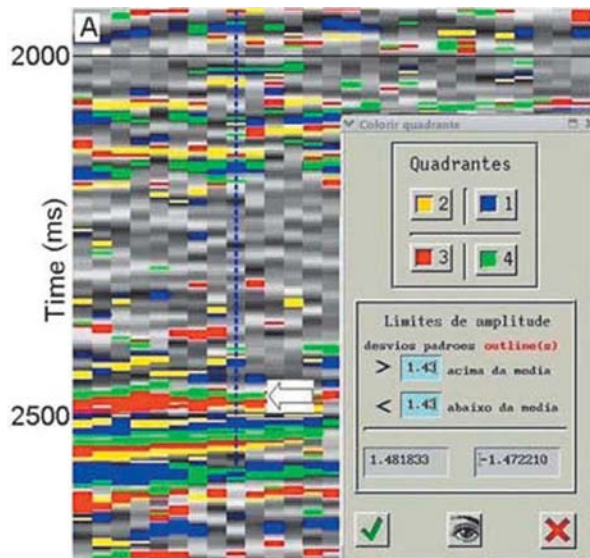
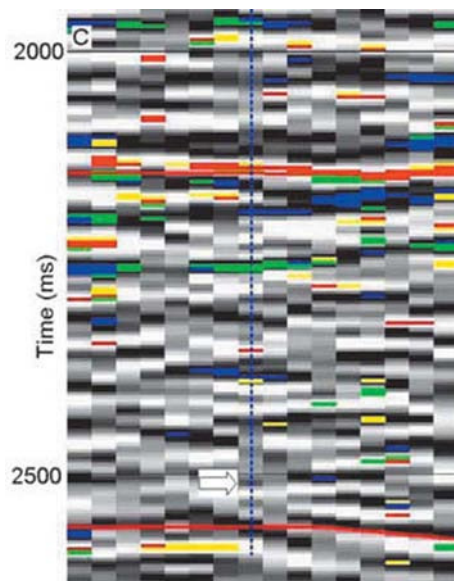
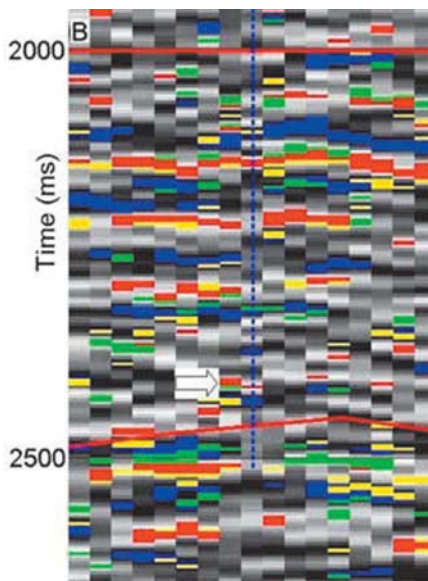


Figure 9. In each orthogonal deviation section a white arrow indicates A) at the top of the FCO a class I anomaly in line 160 B) a weak class I anomaly in line 244 and C) no anomaly in line 28.



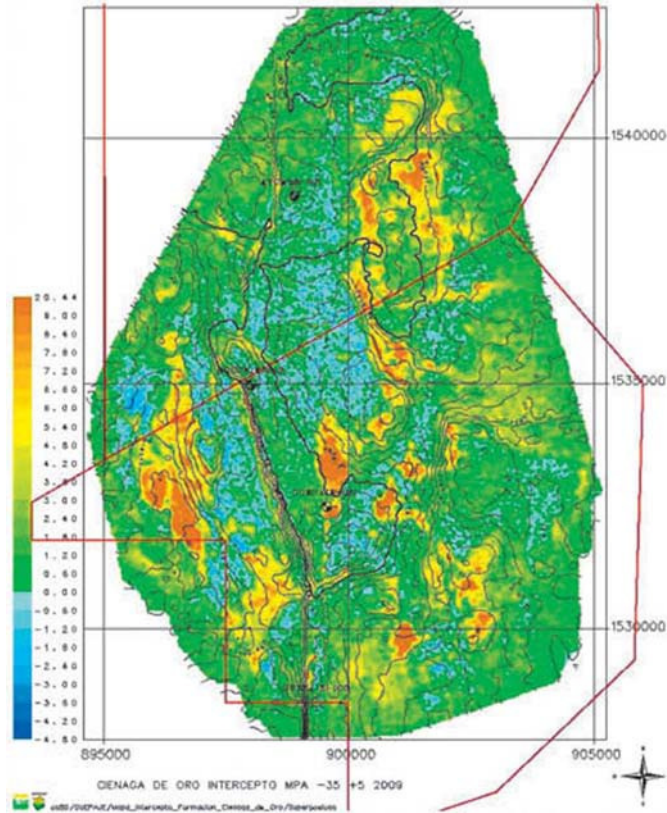
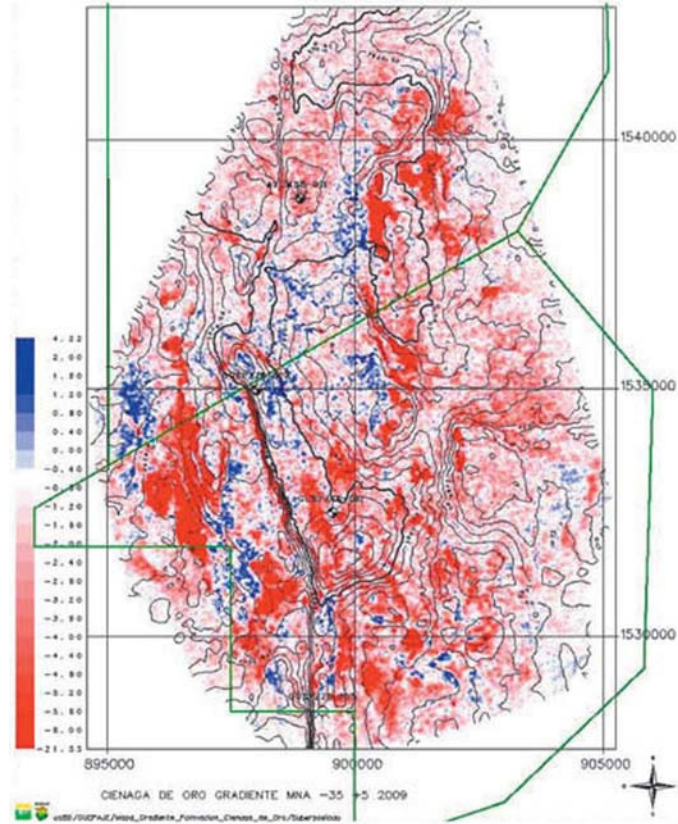


Figure 10. Maps of A) Intercept and B) Gradient at top of the Ciénaga de Oro formation. The bold contour at 2480 ms indicates the gas-water contact.

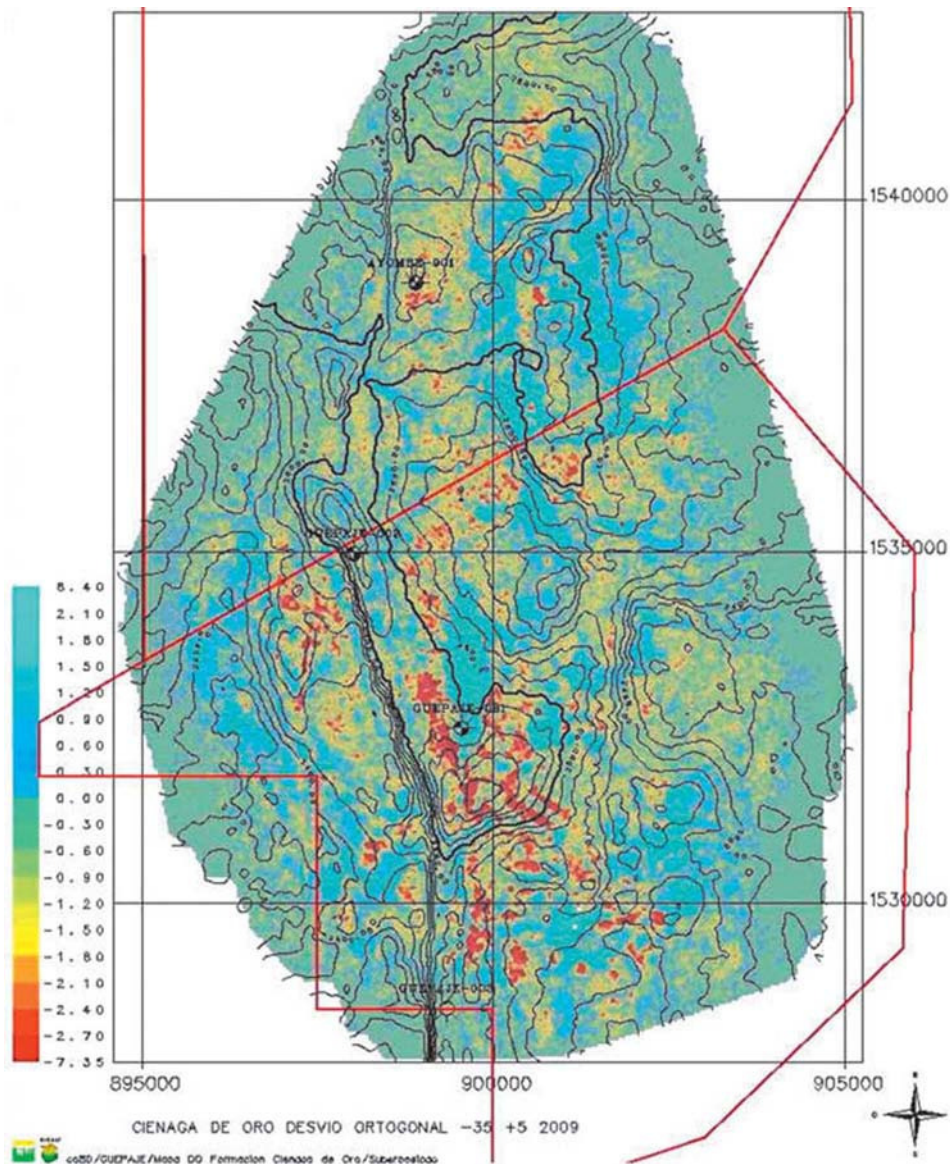


Figure 11. Orthogonal deviation map at top of FCO with the gas-water contact contour in bold at 2480 ms.

presence of negative orthogonal deviation values, with values below -1.6 in Ayombe-1 (-1.88) and Güepajé-1 (-2.66) which can be considered highly anomalous and also values above -1.6 in Güepajé-2 (-1.33) and Güepajé-3 (-0.23) which are closer to the background line.

A structural map of the surface at the top of the FCO was created, enhancing the GWC and shallowest zones, seen in Figure 12A. In order to relate the structural map with the orthogonal anomaly map, another map was created which includes only deviation anomalous values below -1.6, represented by red dots in Figure 12B. In the Ayombe-1 and Güepajé-1 wells the anomalies observed in Figure 12B indicate gas presence which agrees with observed AVO anomalies and

test drilling. Besides, a weak anomaly in the vicinity of Güepajé-2 and no anomaly at Güepajé-3 wells were observed. The correlation between the two maps shows anomalies concentrated in the zone enclosed by 2480 ms curve and in the highest areas of folded surface. Even though, there are deviation anomalies in deep areas of the folded surface.

This adverse result might be due to factors such as influence of lithology, since the top FCO is under a varying thick carbonate level. Therefore, the AVO response would be stronger than by presence of gas. Besides, variable thickness of both partial and full saturated layers in the study area may enforce tuning at the top of the FCO, obscuring the procured results.

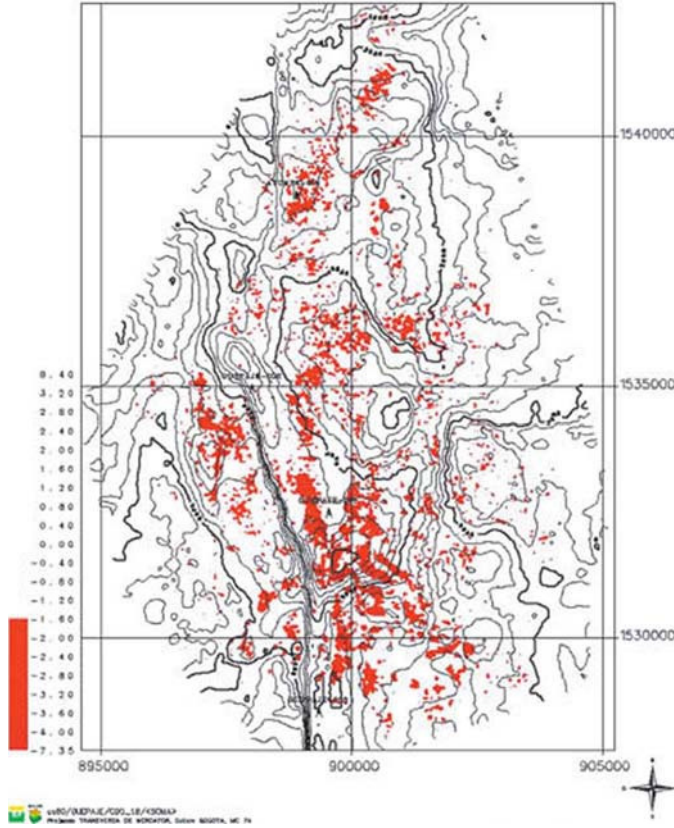
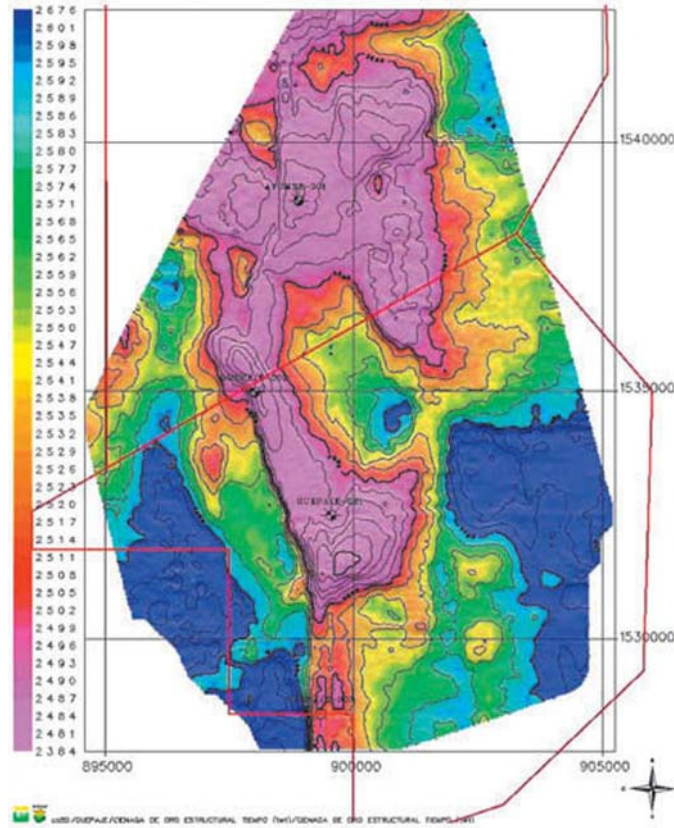


Figure 12. A) Structural map at the top of FCO correlated with B) gas anomaly map.

Conclusions

A class I AVO anomaly was identified at the top of a gas saturated zone in the Ciénaga de Oro formation by AVO modeling of the Ayombe-1 well, that showed that up to 40°, would not have a phase change occur in the presence of gas.

The AVO analysis in four 2D lines which cross or are close to the four wells, found no anomaly in the proven dry Güepajé-3 well, and class I anomalies in the Güepajé-1 and Ayombe-1 gas wells. Even with gas presence, no anomaly was observed in the Güepajé-2 well.

The substitution of gas by water in the Ayombe-1 well provided similar responses, this along with the observed anomalies point out the low sensitivity of AVO analysis for gas detection in this area.

After applied to the seismic volume of the Güepajé-3D Project, the AVO with Partial stack technique provided a gas indicator map which correlated well the structural map of the surface at top of FCO. Some anomalies were observed in zones with low probability of gas presence. This adverse result might be due to lithic factors, e.g. the carbonate layer that overlies the FCO as also the unknown varying thickness distribution in the partially and the fully saturated layers at the top of the FCO.

The technique uses stacked data with a better signal to noise ratio allowing a fast evaluation of possible anomalies in seismic sections and in maps, and besides facilitates to use a direct indicator of hydrocarbons. Its main disadvantage is its minor content of frequency, associated to the NMO stretch and losses by absorption. A dipolar sonic log would provide reliable results by diminishing the uncertainty to estimate shear wave velocity.

Acknowledgments

The authors thank PETROBRAS for the technical support rendered and for the information supplied to the project. Also, thanks to the Universidad Nacional de Colombia where the research was developed. This paper is a product of the Master's thesis in Geophysics of the Geologist Juan C. Mosquera.

Bibliography

Barrero D., Pardo A., Vargas, C., Martínez, J., 2008, Colombian Sedimentary Basins: Nomenclature, Boundaries and Petroleum Geology, New Proposal, Agencia Nacional de Hidrocarburos, Bogotá.

Castagna J., Swan H, 1997, Principles of AVO crossplotting, *The Leading Edge*, 16, 337-342.

Castagna J., Batzle M., Eastwood R, 1984, Relationships between compressional wave and shear wave velocities in clastic silicate rocks, *SEG Expanded Abstracts*, 3, 582-584.

Connolly P, 1999, Elastic impedance, *The Leading Edge*, 18, 438-452.

Gassmann F, 1951, Elastic waves through a packing of spheres, *Geophysics*, 16, 673-685.

Greenberg M., Castagna J., 1992, Shear wave velocity estimation in porous rocks: theoretical formulation, preliminary verification and application, *Geophys. Prosp.*, 40, 195-209.

Hilterman F., 1975, Amplitudes of seismic waves: a quick look, *Geophysics*, 40, 745-762.

Koefoed O., 1955, On the effect of Poisson's ratio of rock strata on the reflection of plane waves, *Geophys. Prosp.*, 3, 381-387.

Maver K., Bolding K., 2004, Simultaneous AVO inversion for accurate prediction of rock properties, *Offshore Technology Conference*, Houston, TX., OTC 16925.

Ostrander W., 1984, Plane - wave reflection coefficients for gas sands at non-normal angles of incidence, *Geophysics*, 49, 1637-1648.

Rosa A., Santos P., Campos R., 1999, AVO analysis with the elastic impedance concept, *VI International Congress of the Brazilian Geophysical Society*, Rio de Janeiro, 3-6.

Rutherford S., Williams R., 1989, Amplitude versus offset variations in gas sands, *Geophysics*, 54, 680-688.

Sánchez J., 1993, Informe Interno Final del Pozo Ayombe-1, Empresa Colombiana de Petróleos - ECOPETROL, 21.

Shuey R., 1985, A simplification of the Zoeppritz equations, *Geophysics*, 50, 609-614.

Smith G., Gidlow P., 1987, Weighted stacking for rock property estimation and detection of gas, *Geophys. Prosp.*, 35, 993-1014.

Wei X., Jiang X., Booth D., Liu Y., 2006, The inversion of seismic velocity using a partial-offset stack with well-log constraints. *J. Geophys. Eng.*, 3, 50-58.